Development 140, 4256-4265 (2013) doi:10.1242/dev.099366

Brinker possesses multiple mechanisms for repression because its primary co-repressor, Groucho, may be unavailable in some cell types

Priyanka Upadhyai and Gerard Campbell*

SUMMARY

Transcriptional repressors function primarily by recruiting co-repressors, which are accessory proteins that antagonize transcription by modifying chromatin structure. Although a repressor could function by recruiting just a single co-repressor, many can recruit more than one, with *Drosophila* Brinker (Brk) recruiting the co-repressors CtBP and Groucho (Gro), in addition to possessing a third repression domain, 3R. Previous studies indicated that Gro is sufficient for Brk to repress targets in the wing, questioning why it should need to recruit CtBP, a short-range co-repressor, when Gro is known to be able to function over longer distances. To resolve this we have used genomic engineering to generate a series of *brk* mutants that are unable to recruit Gro, CtBP and/or have 3R deleted. These reveal that although the recruitment of Gro is necessary and can be sufficient for Brk to make an almost morphologically wild-type fly, it is insufficient during oogenesis, where Brk must utilize CtBP and 3R to pattern the egg shell appropriately. Gro insufficiency during oogenesis can be explained by its downregulation in Brk-expressing cells through phosphorylation downstream of EGFR signaling.

KEY WORDS: Brinker, Groucho, CtBP, Repression, Co-repressor

INTRODUCTION

Transcriptional repressors commonly recruit accessory proteins known as co-repressors (CoRs) that provide them with repressive activity by modifying chromatin structure. CoRs, such as Groucho (Gro) and C-terminal binding protein (CtBP), function as part of complexes containing enzymes that influence transcription by covalently modifying histones and influencing nucleosome packing and the binding of chromatin-associated proteins (Chen et al., 1999; Gromöller and Lehming, 2000; Zhang and Emmons, 2002; Shi et al., 2003; Subramanian and Chinnadurai, 2003; Kim et al., 2005; Winkler et al., 2010). Theoretically, the recruitment of a single CoR could be sufficient for a repressor to silence all of its target genes. However, many repressors can recruit more than one CoR; for example, the *Drosophila* repressors Hairy, Hairless, Knirps and Brinker (Brk) can each recruit CtBP and Gro via conserved 4-10 amino acid CtBP- and Gro-interaction motifs (CiMs and GiMs) (Paroush et al., 1994; Nibu et al., 1998a; Poortinga et al., 1998; Hasson et al., 2001; Zhang et al., 2001; Barolo et al., 2002; Payankaulam and Arnosti, 2009). This ability to recruit both CoRs is somewhat perplexing given that they appear to possess different properties, in particular in respect to the distance over which they can function, with CtBP activity being limited to short distances of ~150 bp from a transcription factor (TF) binding site (Nibu et al., 1998a), whereas Gro can function over a much longer range (Barolo and Levine, 1997; Martinez and Arnosti, 2008); although when recruited by Knirps, Gro has similar short-range properties to CtBP (Payankaulam and Arnosti, 2009). Consequently, it is unclear what CtBP can do that Gro cannot, raising the question of why Gro alone is not sufficient?

Department of Biological Sciences, University of Pittsburgh, Pittsburgh, PA 15260, USA.

*Author for correspondence (camp@pitt.edu)

Accepted 1 August 2013

Possible reasons are as follows. (1) Quantitative: two CoRs may additively provide more repressive activity than can be provided by one alone. (2) Qualitative: one CoR may provide a unique activity that is not provided by the other and which is essential for repression of one or more target genes. Alternatively, a TF may be unable to recruit one CoR at some targets where the other would be required. (3) To minimize noise: a second CoR may serve as a backup to ensure that the TF works efficiently all the time. (4) Availability: each CoR may not be expressed or active in all cells in which the TF functions. Both CtBP and Gro appear to be expressed ubiquitously (Nibu et al., 1998b; Poortinga et al., 1998; Jennings and Ish-Horowicz, 2008) but Gro activity can be downregulated by phosphorylation downstream of receptor tyrosine kinase (RTK) signaling cascades (Hasson et al., 2005; Cinnamon et al., 2008).

Previous studies on the TFs Hairy, Hairless, Knirps and Brk have not been conclusive in uncovering why they possess recruitment motifs for both Gro and CtBP. Most studies reveal that Gro is essential for the repression of at least some targets; for example, reducing Gro levels results in derepression of the Hairless, Hairy, Knirps and Brk targets vg^{QE}, *fushi tarazu*, *even skipped* and *spalt* [*sal*; *spalt major* (*salm*) – FlyBase], respectively (Paroush et al., 1994; Winter and Campbell, 2004; Nagel et al., 2005; Jennings et al., 2008; Payankaulam and Arnosti, 2009). Reducing CtBP levels often has no effect, for example on Brk or Hairless targets in the wing disc (Winter and Campbell, 2004; Nagel et al., 2005), although some Knirps targets and to a lesser extent Hairy targets may show derepression during embryogenesis (Keller et al., 2000; Bianchi-Frias et al., 2004; Struffi and Arnosti, 2005). In some cases, a TF can repress some of its targets even in the absence of both Gro and CtBP, as is the case for the Brk target *optomotor-blind* (*omb*; *bifid* – FlyBase) in the wing disc, indicating that they can use additional mechanisms to repress; Brk has a third repression domain, 3R (Winter and Campbell, 2004). Brk may also recruit a third CoR, Nab, although this does not appear to be required for growth and patterning, but only for Brk-dependent apoptosis induced by reduced Dpp signaling (Ziv et al., 2009).

Overexpression studies reveal that modified TFs only possessing a GiM or a CiM can repress most known targets, at least to some extent, even targets that appear to be dependent on the non-recruited CoR in genetic assays, suggesting that the targets are not CoR specific but that one CoR might provide higher levels of activity in some situations (Struffi et al., 2004; Winter and Campbell, 2004). Exceptions to this include many Hairy targets and the Brk target *tolloid* (*tld*) in early embryogenesis, which only appear to be repressed by proteins possessing a GiM, a CiM being insufficient (Zhang and Levine, 1999; Hasson et al., 2001). Also, the overexpression of Hairless proteins containing only a GiM or a CiM appear to induce different phenotypes during eye development (Nagel and Preiss, 2011).

The approaches described above have several drawbacks, including the following. (1) Analyses have been limited to certain tissues, but each TF functions in many. (2) *CtBP* and *gro* loss of function is difficult to compare with loss of function of a single TF that utilizes both CoRs because of pleiotropic effects as both are utilized by many other TFs. (3) Overexpression is not easily compared with wild-type function, not least because the levels produced rarely mirror that of the endogenous protein. (4) Some TFs may have additional repressive activities that are independent of CtBP and Gro (Winter and Campbell, 2004; Nagel et al., 2005).

The most direct approach to address this issue would be to compare the activity of proteins from mutants in which the CiM and/or the GiM are nonfunctional. Such mutants are not available for any of the four TFs Hairless, Hairy, Knirps and Brk. Consequently, we have generated a series of endogenous *brk* mutants in which the CiM, GiM and 3R are mutated individually or in combination. This was achieved using the genomic engineering approach of Huang et al. (Huang et al., 2009), in which a gene is replaced by an *attP* ΦC31 bacteriophage integration site that allows the insertion of modified/mutated forms that essentially replace the endogenous gene.

We have analyzed the activity of each of these mutants in different tissues in which Brk is known to function, including (1) the early embryo, where it is expressed in the ventrolateral region and restricts expansion of dorsally expressed genes (Jaźwińska et al., 1999a); (2) later embryos, where it is required to establish the characteristic ventral denticle belts of the larva (Lammel et al., 2000; Saller et al., 2002); (3) in the wing disc, where it is expressed in lateral-to-medial gradients and restricts targets to medial regions (Campbell and Tomlinson, 1999; Jaźwińska et al., 1999b; Minami et al., 1999); and (4) during oogenesis, where it is expressed in the follicle cells surrounding the developing oocyte and is required to help pattern the egg shell (Chen and Schüpbach, 2006). We show that Gro is necessary and sufficient for Brk to function in generating a morphologically wild-type fly, although not efficiently. However, Gro is not sufficient for Brk to function during oogenesis, where CtBP and 3R are essential. Here, Brk activity coincides with high levels of RTK signaling that have been shown previously to downregulate Gro activity, making it unavailable for Brk and explaining why it requires additional mechanisms for repression.

MATERIALS AND METHODS

Fly strains and reporter constructs

Flies carrying the following existing alleles or transgenes were used: brk^{F124}, brk^{E427}, brk^{F138}, brk^{M68}, brk^{XA}, gro^{E48}, gro^{MB36}, $CtBP^{l(3)87De\text{-}10}$, gro RNAi (P{TRiP.HMS01506}attP2), hs-GFP (P{hsp70-flp}1, 3 and P{ry[+t7.2]=hsFLP}86E), FRT18A, FRT82B, arm-lacZ, omb-lacZ, w^{1118}, y^{1}, Ras RNAi-Ras85D (P{TRiP.JF02478}attP2), $vasa\Phi C31^{ZH\text{-}102D}$, UAS-GFP, tub>CD2>Gal4, hs-Cre, hs hid, hs-iSceI, Gal4-221[w–], UAS-rl^{SEM}, en-Gal4. The salE1 reporter is a 471 bp fragment at the 3′ end of sal1.8S/E (Kühnlein et al., 1997) cloned into the GFP reporter vector pHSB, which is a modified version of pH-Stinger (Barolo et al., 2000).

Generation of the *brk* knockout strain

This was carried out as described previously (Huang et al., 2008; Huang et al., 2009; Zhou et al., 2012) and is outlined in Fig. 1A and supplementary material Fig. S1.

Generation of *brk* mutants

In vitro generated *brk* mutants have been described previously (Winter and Campbell, 2004). These were cloned into the pGE-$attB^{GMR}$ vector (Huang et al., 2009), injected into the $brk^{KO\text{-}w\text{–}}$ strain expressing ΦC31 integrase and integrations identified as w^{+} transformants. These were validated molecularly (supplementary material Fig. S2) and the w^{+} marker was removed with hs-Cre and revalidated (supplementary material Figs S1, S2, Table S1).

Analysis of protein levels in *brk* mutants

Brk protein levels in mutant cells were compared with that in wild type by antibody staining of wing discs containing mutant clones. After ensuring that the confocal detectors were not saturated, clones were chosen for analysis in the lateral-most regions of the disc (to eliminate any effects from *brk* autorepression in more medial locations) and levels of fluorescence were averaged over the region of a clone using ImageJ (NIH) software and compared with that for an adjacent wild-type twin spot.

Genetic mosaics, overexpression and RNAi-mediated knockdown in the follicular epithelium

Loss-of-function clones were generated by the FRT/FLP recombination technique (Xu and Rubin, 1993). Adult females were heat shocked twice for 1 hour each at 37°C with a 6-8 hour interval between. Eggs were evaluated 5-8 days after heat-shock treatment. To ubiquitously knockdown and upregulate EGFR/Ras/MAPK signaling, Ras85D RNAi and UAS-rl^{SEM} were driven by either CY2-Gal4 or GR1-Gal4 (with similar results), which drive ubiquitous Gal4 in follicle cells of stage 10 egg chambers.

Clonal analysis, overexpression or RNAi-mediated knockdown in the wing imaginal disc

Clones were generated in the second or early third instar in larvae of the following genotypes:

y omb-lacZ brk FRT18A/hsGFP FRT18A; hs-flp;

y omb-lacZ brk FRT18A/arm-lacZ FRT18A; salE1; hs-flp; and

hs-flp; FRT82B $CtBP^{l(3)87De\text{-}10}$ gro^{E48}/FRT82B arm-lacZ.

UAS-rl^{SEM} and gro RNAi were driven with en-Gal4.

RNA *in situ* hybridization, immunohistochemistry and analysis of wings

In situ hybridizations on 2- to 4-hour-old embryos were carried out as described (Tautz and Pfeifle, 1989). *brk* mutants were balanced over FM7c-FtzlacZ and hemizygous embryos were identified by the absence of *lacZ*. Dissection and staining of wing discs were carried out according to standard techniques. Antibodies used were anti-Sal (rabbit, 1:50) (Kühnlein et al., 1994), anti-β-gal (rabbit, 1:2000; Cappel), anti-Brk (1:400) (Campbell and Tomlinson, 1999) and monoclonal anti-Gro (1:2000; Developmental Studies Hybridoma Bank).

Female fertility analysis

Female fertility was evaluated by mating 100 3- to 4-day-old females to 2- to 3-day-old w^{1118} males. After 8-10 days, unfertilized eggs were scored by the absence of nuclei from 5- to 6-hour DAPI-stained embryos. For every genotype indicated three independent experiments were carried out with at least 100 eggs scored.

Imaging and statistical analysis

Confocal imaging was performed on an Olympus Fluoview FV1000. Images were analyzed using ImageJ. All data shown are mean ± s.e.m. Statistical analysis was carried out using GraphPad Prism 6.0 software and

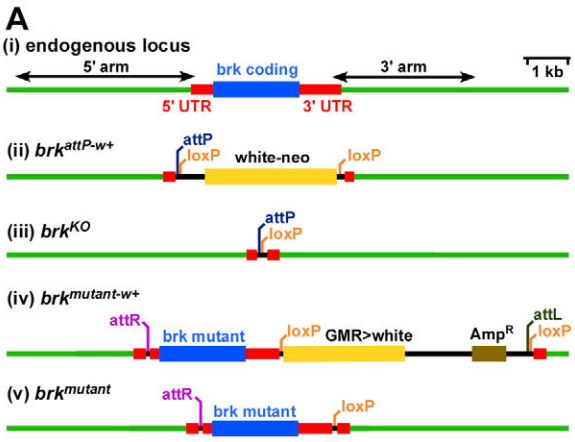

B

	Domains present 3R	CiM	GiM	Viability	Target repression wing	sal	ombZ	Embryo[3]	Denticle belts[4]	Female fertility
wt	+	+	+	AW	+++	+++		+++	wt	wt
KO	-	-	-	EL	-	-		-	xxxx	-
wt rescue	+	+	+	AW	+++	+++		+++	wt	wt
CM	+	-	+	AW	+++	+++		+++	wt	75%
Δ3R[1]	-	+	+	AW	+++	+++		+++	wt	75%
GM	+	+	-	EL	++	++		-	xx	-
Δ3RCM	-	-	+	AW[2]	+++	++		+++	xx	-
Δ3RGM	-	+	-	EL	++	++		-	xxx	-
CMGM	+	-	-	EL	+	+		-	xxx	-
3M	-	-	-	EL	-	-		-	xxxx	-

Fig. 1. The *Drosophila brk* genomic locus in wild type and mutants and summary of mutants. (**A**) *brk* genomic locus. (i) Wild-type locus; note that *brk* has no introns. The 5′ and 3′ homology arms used in the targeting construct (supplementary material Fig. S1) are indicated. (ii) The initial knockout generated, $brk^{attP\text{-}w+}$; the region between the homology arms is replaced by an *attP* site and a *white* gene flanked by *loxP* sites. (iii) brk^{KO}; the *white* gene in $brk^{attP\text{-}w+}$ is eliminated using Cre, resulting in *brk* being replaced with an *attP* and a *loxP* site. (iv) *brk* mutants were integrated into the *attP* site using ΦC31 integrase, the initial constructs having a *white* gene to identify transformants. (v) Final mutants have the *white* gene removed with Cre. (**B**) Wild-type (wt) Brk protein has a DNA-binding domain (DBD) and three independent repression motifs: 3R, a CtBP interaction motif (CiM) and a Gro interaction motif (GiM). See text for details on the assays used to assay the activity of the mutant proteins. AW, adult with wild-type morphology; EL, embryonic lethal. [1]Previously (Winter and Campbell, 2004) this deletion was referred to as NA; [2]few females survive to adult and many males may have slight defects in wing patterning; [3]*dpp*, *tld*, *zen*; [4]severity of loss of ventral embryonic denticles in first instar larvae (xxxx, most severe). For target repression, '-' indicates no repression; for female infertility, '-' indicates fertility not tested owing to embryonic lethality. Gray plus sign indicates variable result.

statistical significance was tested using the Mann-Whitney U test, chi-square test for trend, or the Kruskal-Wallis multiple comparison test.

RESULTS

Generation of endogenous *brk* mutants

To create endogenous *brk* mutants we followed the genomic engineering technique of Huang et al. (Huang et al., 2009). First, using their extension of the knockout technique of Golic and colleagues (Rong and Golic, 2000; Gong and Golic, 2003; Huang et al., 2008), the *brk* gene was replaced with a minimal ΦC31 bacteriophage *attP* site and a *white* (w^+) marker flanked by *loxP* sites to create the $brk^{attP\text{-}w+}$ allele (Fig. 1A; supplementary material Fig. S1). Cre recombinase was then used to remove the *w*+ marker and create the *brk* knockout allele brk^{KO}. Second, DNA constructs containing a minimal *attB* site, a w^+ marker flanked by *loxP* sites and a wild-type *brk* gene or one of a series of mutants in which the 3R, CiM and GiM elements were mutated or deleted individually or in combination, was integrated into the *attP* site of brk^{KO} (Fig. 1B; supplementary material Fig. S1). The w^+ marker was then removed using Cre, resulting in strains carrying either wild-type or mutant *brk* genes that, apart from the mutations, differ from the native locus only by possessing an *attR* site (50 bp) and a *loxP* site (34 bp) in the 5′ UTR and 3′ UTR, respectively.

Validation of brk^{KO} and integrated *brk* mutants

The identity of the brk^{KO} allele was confirmed as follows. (1) Molecularly: by restriction mapping and sequencing of amplified genomic DNA (supplementary material Fig. S2). (2) Genetically: the allele is phenotypically indistinguishable from known null alleles, with a characteristic embryonic denticle phenotype (see below) and enlarged wing phenotype over a viable hypomorph (supplementary material Fig. S3). (3) Protein levels: protein is undetectable in brk^{KO} homozygous wing disc clones (Fig. 2A; supplementary material Fig. S4); this indicates that there is very little, if any, perdurance of wild-type protein in mutant clones. (4) Rescue: viability is restored following integration of a wild-type gene into the *attP* site. The resultant brk^{rescue} allele is functionally wild type, and protein levels in wing clones are comparable to those in adjacent wild-type twin spots (Fig. 2B; supplementary material Figs S3, S4).

The *brk* mutant alleles were then similarly characterized molecularly and confirmed to carry the expected mutations (supplementary material Fig. S2). The levels of mutant proteins in clones were compared with that in adjacent wild-type twin spots and were all found to be equivalent, including brk^{3M}, in which all three repression domains/motifs are eliminated (Fig. 2C; supplementary material Fig. S4). Consequently, any differences in the activity of the different mutant proteins cannot be attributed to variations in protein stability. A summary of the mutants generated in this study and their activity is shown in Fig. 1B.

We then validated the alleles genetically. Based on previous *in vitro* studies the brk^{GM} and brk^{CM} mutants are predicted to be unable to recruit Gro and CtBP, respectively (Hasson et al., 2001; Zhang et al., 2001). To confirm this genetically we used a *sal* reporter, salE1, as a target in the wing disc [note that its expression is not dependent upon Omb, unlike endogenous *sal* (del Álamo Rodríguez et al., 2004)]. salE1-GFP expression is restricted to medial regions of the disc by Brk: it is derepressed in *brk* null clones laterally (Fig. 2E). Analysis of *CtBP* and *gro* single- and double-mutant clones revealed that salE1-GFP expression is derepressed only when both are removed, indicating that at least one is necessary and either is sufficient to provide Brk with repressive activity to silence salE1 (Fig. 2F-H). In agreement, salE1 is derepressed in brk^{CMGM} clones but not brk^{GM} clones or brk^{CM} discs (Fig. 2I-N; this mutant is viable, see below), but salE1 is derepressed in brk^{CM} discs when *gro* is downregulated by RNAi (Fig. 2J); *gro* RNAi does not induce derepression of salE1 in wild-type or $brk^{\Delta 3R}$ discs (not shown; Fig. 2L). This supports Brk^{CM} and Brk^{GM} being unable to recruit CtBP and Gro, respectively, whereas they can recruit the other, while Brk^{CMGM} cannot recruit either.

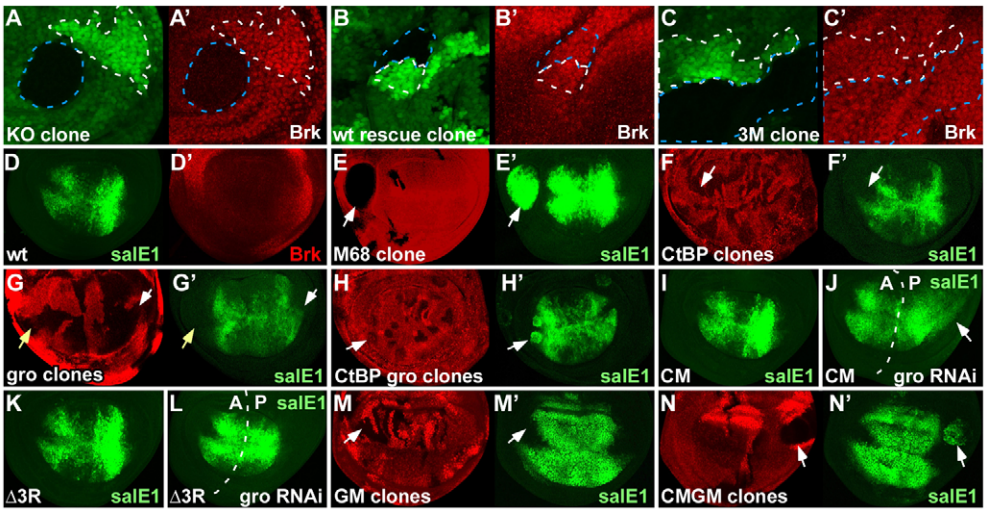

Fig. 2. Validation of endogenous *brk* mutants. Third instar wing discs are shown with anterior to the left. (**A-C′**) Discs containing homozygous mutant clones (identified by loss of ubiquitous marker, green; blue outline) immunostained for Brk (red); adjacent twin spot is outlined in white. (A,A′) brk^{KO} clone. (B,B′) brk^{rescue} clone. (C,C′) brk^{3M} clone. (**D**,**D′**) salE1-GFP and Brk in wild-type discs. (**E**,**E′**) brk^{M68} null mutant clone shows strong derepression of salE1 laterally (arrows). (**F**,**F′**) salE1 expression is unaffected in *CtBP* mutant clones. (**G**,**G′**) Some *gro* clones show minor derepression of salE1 (white arrows) but others do not (yellow arrow). (**H**,**H′**) salE1 is strongly derepressed in *CtBP gro* double-mutant clones (arrows). Note that there is derepression of salE1 outside of the pouch, unlike brk^{M68} mutant clones, which we assume to be due to another TF repressing salE1 in lateral regions and requiring CtBP or Gro. (**I**) In brk^{CM} mutant discs salE1 appears as in wild type (D). (J,L) *gro* RNAi in posterior (anterior-posterior boundary indicated). (**J**) salE1 is expanded (arrow) following *gro* knockdown in brk^{CM} hemizygotes. (**K-M**) salE1 is wild type in $brk^{\Delta 3R}$ discs (K), in $brk^{\Delta 3R}$ discs following *gro* knockdown (L) and in brk^{GM} mutant clones (M). (**N**) salE1 is strongly derepressed (arrow) in brk^{CMGM} clones.

Gro recruitment, but not CtBP or 3R, is necessary to generate adult flies

Previous indications that Gro is the primary CoR for Brk (Winter and Campbell, 2004) were confirmed by our mutant analysis. Like nulls, any allele in which the GiM is mutated is embryonic lethal, including brk^{GM} in which the CiM and 3R remain intact, indicating that Gro recruitment is indispensable for Brk function (Fig. 1B). By contrast, brk^{CM} and $brk^{\Delta 3R}$ adults are morphologically wild type (Fig. 3A-C), and even some $brk^{\Delta 3RCM}$ mutants, which have Gro as their primary repressive activity, can survive to adults with an almost wild-type phenotype (Fig. 3D). However, $brk^{\Delta 3RCM}$ mutants display a high degree of lethality, in particular among females, with most dying at the end of embryogenesis or as early larvae, and although those that survive appear superficially wild type, more detailed analysis indicates that their wings have a posterior enlargement or even a fused alula (Fig. 3D,E; supplementary material Fig. S5). Thus, Gro is necessary and almost sufficient alone to provide Brk with the activity to take a fly from fertilization to adult, but CtBP or 3R is required to ensure that this happens consistently, even if, individually, each appears dispensable for generating an adult fly.

Regulation of wing targets in *brk* mutants

sal and *omb* have both been shown to be direct targets of Brk in the wing (Sivasankaran et al., 2000, Barrio and de Celis, 2004) and we assessed the ability of mutant proteins to repress them, again using clonal analysis. This assumes that we are assessing only mutant protein activity, i.e. that no wild-type protein perdures in the clones. As already pointed out, this is supported by the fact that no protein is detected in brk^{KO} clones by antibody staining (Fig. 2A) and is also backed up by the observation that *brk* targets are completely repressed in all null clones in the appropriate position in wing discs (Fig. 4A,B). Endogenous *sal* was monitored, in addition to the salE1 analysis reported above, in order to compare with previous results, but, as already noted, there is added restriction to the derepression of endogenous *sal* expression because, unlike salE1, this is dependent on *omb* (del Álamo Rodríguez et al., 2004). brk^{KO} and brk^{3M} mutant clones behave identically to those of previous null alleles showing strong *sal* and ombZ (a *lacZ* enhancer trap) derepression, with ectopic *sal* but not ombZ being restricted to the wing pouch (Fig. 4A,B).

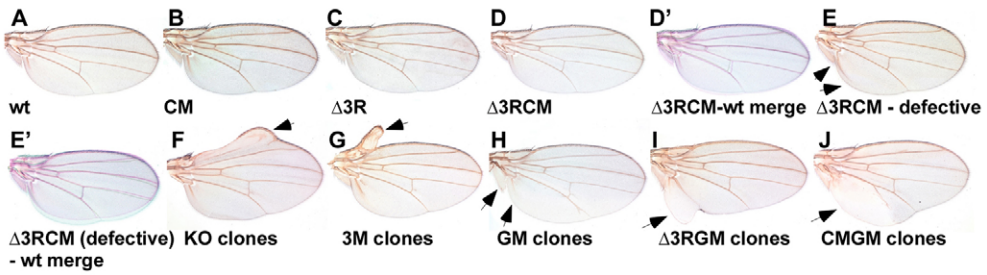

Fig. 3. Adult wings from *brk* mutants. (**A**) Wild type. (**B**,**C**) brk^{CM} (B) and $brk^{\Delta 3R}$ (C) wings are morphologically wild type. (**D**) $brk^{\Delta 3RCM}$ with an almost wild-type wing. (**E**) $brk^{\Delta 3RCM}$ with enlarged wing and fused alula (arrow). (**D′**,**E′**) Comparison with wild type. (**F-J**) Wings from heterozygotes carrying homozygous mutant clones of brk^{KO} (F), brk^{3M} (G), brk^{GM} (H), $brk^{\Delta 3RGM}$ (I) and brk^{CMGM} (J) (clones arrowed).

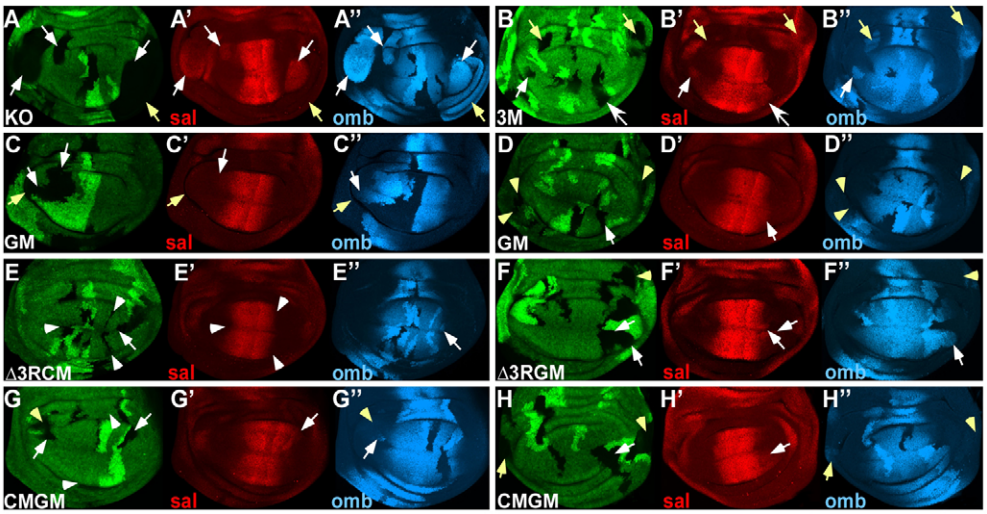

Fig. 4. *sal* and *omb-lacZ* (ombZ) expression in *brk* mutants. Third instar wing discs containing mutant clones immunostained for ombZ (β-gal antibody; note that *omb* is on the same chromosome as *brk* so expression is lost in twin spots) and Sal. (**A-B″**) brk^{KO} and brk^{3M} clones. *sal* and ombZ are both strongly derepressed in the wing pouch/hinge (white arrows) while ectopic ombZ extends outside (yellow arrows). (**C-D″**) brk^{GM} clones. *sal* and ombZ are derepressed close to their endogenous domain (white arrows) but not more laterally within (yellow arrows) or outside the wing pouch/hinge (yellow arrowheads). (**E-E″**) $brk^{\Delta 3RCM}$ clones. *sal* is not derepressed (arrowheads) but minor upregulation of ombZ is noted (arrows). (**F-F″**) In $brk^{\Delta 3RGM}$ clones located mediolaterally, both *sal* and ombZ are derepressed (white arrows) but no ectopic expression is seen outside the wing pouch/hinge (yellow arrowheads). (**G-H″**) brk^{CMGM} clones. (G-G″) *sal* is derepressed within the wing pouch (white arrows) and ombZ is derepressed close to its endogenous domain but not more laterally (yellow arrowheads). (H-H″) Sometimes ombZ is derepressed outside the wing pouch/hinge (yellow arrow) but not always (yellow arrowheads).

The $brk^{\Delta 3RCM}$, $brk^{\Delta 3RGM}$ and brk^{CMGM} mutants will reveal the sufficiency of a single factor to provide Brk with repressive activity, namely Gro, CtBP and 3R, respectively. In $brk^{\Delta 3RCM}$ clones *sal* shows no derepression, whereas ombZ can show derepression but only very close to the endogenous domain, indicating that Gro alone provides sufficient activity to fully repress *sal* and almost enough to fully silence ombZ (Fig. 4E). By contrast, although CtBP alone also provides some activity to repress both targets, which are fully repressed in clones in lateral regions, it is far from sufficient as there is some *sal* and ombZ derepression in more medial clones close to the endogenous domains (Fig. 4F). 3R alone provides some activity but is even less sufficient, with brk^{CMGM} clones showing more extensive derepression of both *sal* and ombZ within the wing pouch and ombZ occasionally, but not always, outside of the pouch (Fig. 4G,H). This derepression of ombZ in brk^{CMGM} is a little surprising as this was not observed in *CtBP gro* double-mutant clones or in the brk^{F138} mutant, which encodes a truncated protein eliminating CiM and GiM (Winter and Campbell, 2004). The reason for this is unclear. This double-mutant analysis reveals that CtBP and 3R can individually provide some activity but are not sufficient for full repression of wing targets, whereas Gro is sufficient for *sal* but not quite for ombZ.

sal and ombZ expression is normal in discs from brk^{CM} and $brk^{\Delta 3R}$ mutants (supplementary material Fig. S6), as would be expected as they survive to adults with wild-type wings, indicating that neither CtBP nor 3R is required for repression of these targets. However, Gro is necessary as both targets are derepressed in brk^{GM} clones, but only close to the endogenous domains (Fig. 4C). In this respect, brk^{GM} is less severe than either brk^{CMGM} or $brk^{\Delta 3RGM}$, indicating that CtBP and 3R together provide Brk with more activity than either alone in the absence of Gro. This is backed up by analysis of clones in adults: brk^{KO}, brk^{3M}, brk^{3RGM} and brk^{CMGM} clones resemble those previously obtained with null alleles, being associated with outgrowths in the proximal anterior and posterior; however, although brk^{GM} clones are associated with some minor effects on vein patterning they never result in significant outgrowths (Fig. 3F-J).

Gro is necessary and sufficient during early embryogenesis but not quite in later embryos

In early embryos *brk* is expressed ventrolaterally and restricts expression of the dorsally expressed genes *dpp*, *tld* and *zen* (Jaźwińska et al., 1999a). As expected, their expression is expanded in brk^{KO} embryos, but this is also true for brk^{GM} embryos, which are indistinguishable from brk^{KO} (Fig. 5A-C). By contrast, expression of these targets appears normal in $brk^{\Delta 3RCM}$ embryos (Fig. 5D). Thus, Gro is required and sufficient for Brk activity in early embryogenesis.

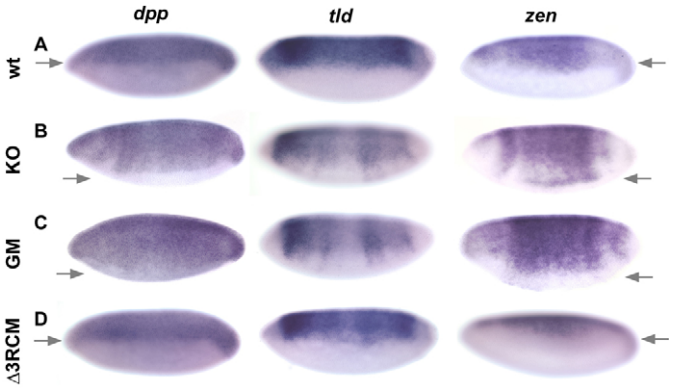

Fig. 5. Expression of Brk targets in early embryogenesis. *In situ* hybridization for *dpp*, *tld* and *zen* in (**A**) wild type, (**B**) brk^{KO}, (**C**) brk^{GM} and (**D**) $brk^{\Delta 3RCM}$ cellular blastoderm embryos; dorsal is up. Arrows indicate the ventral limit of expression.

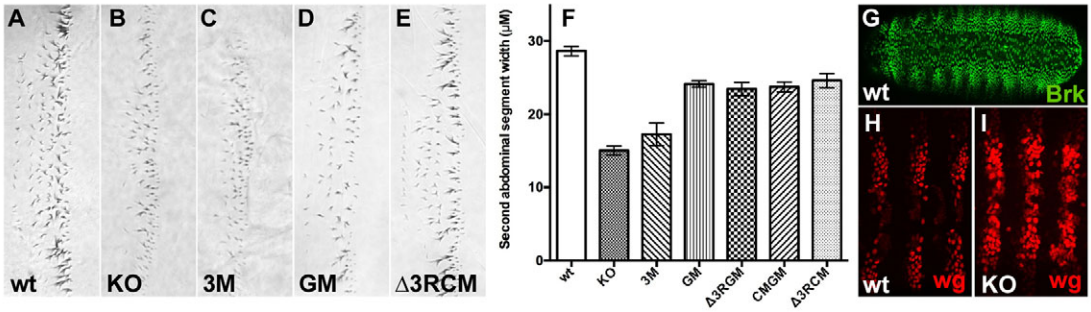

Fig. 6. Patterning the ventral denticle belts (VDBs). (**A-E**) Second VDB from (A) wild type, (B) brk^{KO}, (C) brk^{3M}, (D) brk^{GM} and (E) $brk^{\Delta 3RCM}$ first instar larvae. (**F**) The width of the VDB in the various mutants; each is significantly narrower than wild type. n=10; P<0.01, Mann-Whitney U test; error bars indicate s.e.m. (**G-I**) Ventral ectoderm in stage 12-13 embryos. (G) *brk* (*lacZ*) expression in wild type. (H,I) *wg* (*lacZ*) expression in (H) wild type and in (I) brk^{KO}.

Brk is also required later in embryogenesis in the abdominal epidermis where it helps to establish the repeating pattern of ventral denticle belts (VDBs). Each belt is formed in the anterior region of each segment and is composed of six rows of denticles, with those in rows 1 and 4 pointing anteriorly, whereas the rest point posteriorly (Saller et al., 2002). The VDBs in *brk* null mutants are severely reduced and exhibit a polarity defect with all remaining denticles pointing posteriorly (Jaźwińska et al., 1999a; Lammel et al., 2000; Saller et al., 2002). Both brk^{KO} and brk^{3M} have this null phenotype, but it is slightly less severe in brk^{GM}, with the VBDs being wider than in the nulls, although all remaining denticles point posteriorly (Fig. 6B-D; supplementary material Fig. S7). This indicates that although Gro is required for Brk activity in the ventral embryonic ectoderm it cannot be the only factor providing activity, indicating that CtBP and the 3R domain play a role. Consistent with this, $brk^{\Delta 3RCM}$ mutants also display a mild cuticle phenotype, with some loss of denticles from the first three rows but the polarity of the remaining denticles being normal (Fig. 6E; supplementary material Fig. S7); this also indicates that Gro is insufficient in this regard.

Denticle formation is promoted by EGFR signaling via Rhomboid (Rho)-mediated processing of the Spitz ligand and is antagonized by Wingless (Wg) signaling with *rho* and *wg* being expressed in single stripes per segment (Bejsovec and Martinez Arias, 1991; Golembo et al., 1996; Szüts et al., 1997; Alexandre et al., 1999; Lee et al., 2001). How Brk impacts this is unknown, but our analysis has revealed that the stripes of *wg* expression are expanded in brk^{KO} embryos (Fig. 6H,I), suggesting that *wg* might be an indirect Brk target in the ventral ectoderm. Brk is ubiquitously expressed in the ventral ectoderm (Fig. 6G), so how it spatially restricts *wg* remains to be determined. It is very unlikely that this phenomenon has any link to the recent suggestion that Brk represses *naked cuticle* (*nkd*) in the wing (Yang et al., 2013), the product of which negatively regulates Wg signaling in the embryo (Zeng et al., 2000), because if Nkd was upregulated in *brk* mutants this would lead to phenotypes similar to those of *wg* mutants, whereas *brk* mutants phenocopy *wg* gain of function.

Gro is not sufficient for Brk-mediated patterning of the egg shell during oogenesis

Although brk^{CM} and $brk^{\Delta 3R}$ mutants are viable, fertility studies reveal that Brk activity is compromised as mutant mothers lay a significant percentage of unfertilized eggs: 29% in brk^{CM} and 23% in $brk^{\Delta 3R}$ compared with only 5% in wild type (Fig. 7A). As very few $brk^{\Delta 3RCM}$ females survive to adulthood we were unable to assess fertility in this double mutant. To explain the reduced fertility in the single mutants we analyzed the morphology of the eggs that they laid. Key features of *Drosophila* eggs are located in the dorsal anterior: the dorsal appendages, which are a pair of tubes that aid in respiration, the operculum, which is a lid-like structure through which the larva hatches, and the micropyle, which is an anterior cone-shaped structure that allows sperm entry (Berg, 2005). These structures are patterned during oogenesis by the overlying follicle

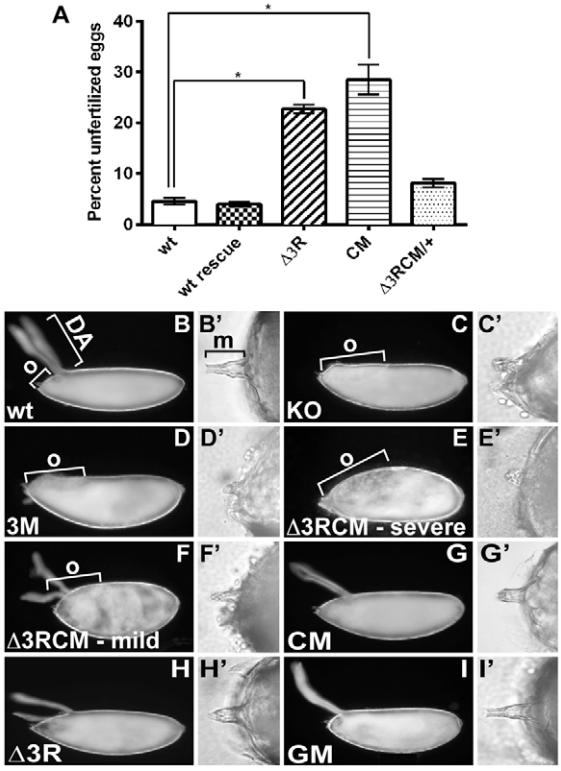

Fig. 7. Female fertility and egg morphology in *brk* mutants. (**A**) Compared with wild type, brk^{CM} and $brk^{\Delta 3R}$ mothers lay significantly more unfertilized eggs, whereas brk^{rescue} and $brk^{\Delta 3RCM}$/+ mothers do not (n=3, *P<0.05, Mann-Whitney U test); error bars indicate s.e.m. (**B-I'**) Eggs showing dorsal appendages (DA) and operculum (o) (B-I) and magnification of anterior showing micropyle (m) (B'-I') from wild-type mothers (B,B'), mothers carrying brk^{KO} mutant clones (C,C'), mothers carrying brk^{3M} mutant clones (D,D'), mothers carrying $brk^{\Delta 3RCM}$ mutant clones (E-F'; F is less severe than E), brk^{CM} mothers (G,G'), $brk^{\Delta 3R}$ mothers (H,H') and mothers carrying brk^{GM} mutant clones (I,I').

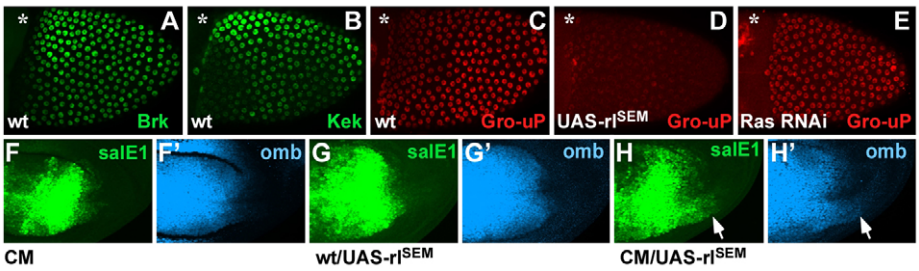

Fig. 8. Gro phosphorylation by EGFR signaling in the follicular epithelium and the third instar wing disc. (**A-E**) Stage 10 egg chambers, anterior left, dorsal up; asterisk marks the dorsal anterior. (A) In wild type, *brk* (*lacZ*) is expressed in a gradient with highest levels in the dorsal anterior follicle cells. (B) *kek* (*lacZ*), a reporter of EGFR/MAPK signaling, is expressed in a similar gradient. (C) An antibody largely specific to the unphosphorylated form of Gro (Gro-uP) shows reduced staining levels in the dorsal anterior. Upregulation (D; UAS-rl^{SEM}/GR1-Gal4) and downregulation (E; Ras85D-RNAi/CY2-Gal4) of Ras/MAPK signaling leads to loss or to uniform levels of unphosphorylated Gro, respectively. (**F-H'**) Posterior region of the wing pouch from third instar wing discs showing ombZ (blue) and salE1-GFP. (F,F') In *brk*^{CM}, expression of both targets is restricted to the medial region. (G,G') This is also the case for wild-type discs in which MAPK signaling has been upregulated (UAS-rl^{SEM}/en-Gal4). (H,H') However, upregulation of MAPK signaling in *brk*^{CM} discs results in lateral expansion of both salE1 and ombZ (arrow).

cells, where *brk* is expressed at high levels in the dorsal anterior (Fig. 8A). Follicle cell clones of *brk* null alleles result in eggs in which the operculum is enlarged and the dorsal appendages are lost (Chen and Schüpbach, 2006; Shravage et al., 2007). The same egg phenotypes were obtained with *brk*^{KO} and *brk*^{3M} mutant clones, but we also identified the additional phenotype of a reduced micropyle, indicating that Brk activity is also required for patterning this structure (Fig. 7C,D; supplementary material Fig. S8).

Eggs laid by *brk*^{CM} and *brk*$^{\Delta 3R}$ mothers exhibit similar but milder egg shell defects including significantly shorter dorsal appendages and a shorter micropyle, the latter possibly accounting for the reduced fertilization rates (Fig. 7G,H; supplementary material Fig. S8). For *brk*$^{\Delta 3RCM}$ we generated follicle cell clones that resulted in eggs with more severe phenotypes than from single-mutant mothers and often approached the severity obtained with null clones, including an enlarged operculum and loss of dorsal appendages, although the phenotype was more variable (Fig. 7E,F; supplementary material Fig. S8). This suggests that 3R and CtBP provide most Brk-mediated activity during oogenesis. Consistent with this, *brk*^{GM} follicle cell clones result in eggs that appear almost wild type, with only a very mild expansion of the operculum, normal dorsal appendages and micropyle (Fig. 7I; supplementary material Fig. S8), indicating that Gro provides little activity for Brk during oogenesis. In contradiction of this, *gro* clones can result in eggs with more severe patterning defects, including reduced dorsal appendages and a reduced micropyle (supplementary material Fig. S8). However, the fact that this is not mirrored by the *brk*^{GM} analysis suggests that Gro is utilized by other TFs in egg patterning that presumably have a lower threshold requirement for Gro.

Gro is phosphorylated and potentially unavailable for Brk function during oogenesis

We next addressed the question of why Gro might not be sufficient to provide Brk with activity during oogenesis. Given that Gro activity can be downregulated by MAPK phosphorylation (Hasson et al., 2005; Cinnamon et al., 2008), we examined Brk expression, EGFR signaling activity and Gro phosphorylation during oogenesis. Initially, we confirmed previous studies showing that *brk* expression and EGFR signaling [as monitored by *kek* (*kek1* – FlyBase) expression] are highest in the dorsal anterior follicle cells of stage 10 egg chambers (Fig. 8A,B; supplementary material Fig. S9). Using an antibody that primarily recognizes the active, unphosphorylated form of Gro (Cinnamon et al., 2008), we find that its staining mirrors that of *kek*, with markedly reduced levels in the dorsal anterior consistent with Gro being phosphorylated and its activity levels reduced here (Fig. 8C; supplementary material Fig. S9). We confirmed that EGFR signaling is controlling the patterns of Gro phosphorylation by upregulating and downregulating signaling levels, with the former resulting in ubiquitously reduced antibody staining and the latter increased staining (Fig. 8D,E; supplementary material Fig. S9).

Thus, Gro may be unavailable for Brk in dorsal anterior follicle cells due to phosphorylation downstream of EGFR signaling. Here, CtBP and 3R provide Brk with repressive activity. Because no direct targets of Brk have been identified in the follicle cells it has not been possible to directly test this model in this tissue, but, if correct, this would predict that upregulating EGFR signaling in other tissues would compromise Brk activity if it were unable to recruit CtBP. We tested this possibility in the wing disc. Above we show that Brk^{CM} is sufficient to repress salE1 here, but reducing Gro activity in this mutant using RNAi results in its derepression (Fig. 2I,J). Similarly, we find that upregulation of EGFR signaling in *brk*^{CM} wing discs using UAS-rl^{SEM} results in derepression of salE1 and also ombZ; this does not occur in wild-type discs (Fig. 8F-H). This is consistent with EGFR signaling reducing Gro availability for Brk.

DISCUSSION

Brk uses Gro as its primary CoR but CtBP and 3R are required in some tissues

Here we have performed a structure/function analysis of the transcriptional repressor Brk by replacing the endogenous *brk* gene with a ΦC31 bacteriophage *attP* site into which mutant forms of *brk* were introduced by integrase-mediated transgenesis (Huang et al., 2009). Our goal was to generate mutations that disrupted the ability of Brk to recruit the CoRs Gro and CtBP and/or that deleted the less well characterized 3R repression domain and to test their activity in different tissues at different times of development to determine if and why they are required by Brk to repress transcription. Previous studies with Brk and other TFs that can recruit both CoRs indicated that Gro recruitment is essential for at least some of the activities of these TFs, but the reason for recruiting CtBP has proven more elusive. Here we have confirmed that Gro recruitment is essential for Brk activity, but have also shown that Brk needs to recruit CtBP and to possess the 3R domain for full activity in some tissues, in particular during oogenesis.

Availability: the key reason why Brk cannot rely on Gro

Lethality of the brk^{GM} mutant reveals Gro recruitment to be necessary for Brk activity. The $brk^{\Delta 3RCM}$ mutant, which utilizes Gro as its sole repressive activity, can progress from fertilization to an almost morphologically wild-type adult, indicating that Gro is close to sufficiency in this regard (Fig. 3D,E). However, $brk^{\Delta 3RCM}$ mutants often die as embryos and show defective oogenesis, with eggs having aberrant egg shell pattering, a characteristic of *brk* null mutants (Fig. 7C-E). The single mutants, $brk^{\Delta 3R}$ and brk^{CM}, show less severe egg shell defects and reduced fertility, the latter probably relating to a defective micropyle, the structure through which sperm normally enter (Fig. 7A-H). The apparent inactivity of $Brk^{\Delta 3RCM}$ protein in follicle cells appears to be explained by active, unphosphorylated Gro being reduced there. The egg shell is patterned by the surrounding follicle cells, where Brk is expressed at high levels in the dorsal anterior (Fig. 8A). This coincides with high levels of EGFR signaling (Fig. 8B) and previous studies have shown that Gro activity is attenuated following phosphorylation by MAPK downstream of EGFR signaling (Hasson et al., 2005; Cinnamon et al., 2008). As expected, we find lower levels of unphosphorylated or active Gro in the dorsal-anterior follicle cells (Fig. 8C). Consistent with the activity of $Brk^{\Delta 3RCM}$ being compromised by EGFR-dependent downregulation of Gro activity, upregulation of EGFR signaling in the wing disc of brk^{CM} mutants results in derepression of the targets salE1 and ombZ (Fig. 8F-H).

EGFR signaling also probably reduces the levels of active Gro available for Brk in other tissues, including the ventral ectoderm where Brk activity is required to ensure proper patterning of the denticle belts and where EGFR signaling is known play a key role (Sanson, 2001). Many $brk^{\Delta 3RCM}$ mutants do not survive embryogenesis and demonstrate defects in denticle patterning similar to, but weaker than, those of null mutants (Fig. 6B-E). In addition, the VDB phenotype of brk^{GM} mutants (Fig. 6D) is less severe than in brk^{KO} or brk^{3M} mutants (Fig. 6B,C). Thus, CtBP and 3R appear to provide repressive activity in the ventral ectoderm.

No Brk targets have been characterized in the follicle cells, but we would expect these to be partially derepressed in both brk^{CM} and $brk^{\Delta 3R}$ mutants and possibly completely derepressed in $brk^{\Delta 3RCM}$ mutants based on the egg shell phenotypes, although there might be some differences between brk^{CM} and $brk^{\Delta 3R}$ given the differences between CtBP and 3R just discussed. However, again, this would not imply that these targets are CtBP/3R specific, because the inability of Gro to participate in their repression is presumed to be due to its unavailability. Thus, although studies have indicated that TFs that have the ability to recruit both Gro and CtBP may only recruit one or other at specific targets (Bianchi-Frias et al., 2004), this might not reflect a CoR specificity for individual targets, but rather a cell-specific availability of CoRs.

Implications of phosphorylation-dependent attenuation of Gro

It is possible that if Gro were available in all cells then the CiM and 3R domain would be dispensable and so, at least for Brk, downregulation of Gro by MAPK phosphorylation could be considered inconvenient. This might be true for other TFs, including Hairy, Hairless and Knirps, which also function in multiple tissues, many of which are exposed to RTK signaling, and might explain why these TFs need to resort to recruiting CtBP as well as Gro (Nagel and Preiss, 2011). It should also be noted that Gro activity can be downregulated in other ways, including phosphorylation by Homeodomain-interacting protein kinase (Choi et al., 2005). This downregulation of Gro activity has been explained in terms of reducing the activity of specific repressors in specific tissues, such as E(Spl) factors during wing vein formation (Hasson et al., 2005; Orian et al., 2007). This appears to be a somewhat illogical way to downregulate the activity of specific repressors, as there are almost certainly many other TFs utilizing Gro in the same cells and in other tissues exposed to RTK signaling and their activity might be compromised. There are no data indicating whether the downregulation of Gro activity in follicle cells serves any purpose and could simply be a consequence of the decision to downregulate Gro activity by this means in other tissues. However, this has serious implications for Brk and has required Brk to be versatile in its mechanisms of repression. Of course, we have not ruled out the possibility that downregulation of Gro activity does serve a purpose for Brk in follicle cells; for example, if Gro were available here it might provide Brk with too much activity or allow it to inappropriately repress a target that CtBP or 3R cannot. This might be tested by assessing egg shell phenotypes after driving unphosphorylatable Gro at physiological levels in a $brk^{\Delta 3RCM}$ mutant, but currently this is technically challenging.

CoR availability as a general explanation for versatility of repression mechanisms by TFs

The idea that repressors need to be versatile in their repressive mechanisms because of variable CoR availability presumably extends beyond Brk and Hairless, Hairy and Knirps. In fact, other repressors in *Drosophila* possess both CiMs and GiMs, including Snail (our unpublished observations). This might not be simply related to downregulation of Gro activity, as CtBP activity can also be modulated; for example, SUMOylation and acetylation of mammalian CtBPs is implicated in regulating their nuclear localization (Lin et al., 2003; Zhao et al., 2006). In addition, other CoRs might similarly be available only in some cells; MAPK activity has been shown to phosphorylate and lead to the nuclear export and inactivation of the SMRT CoR complex (Hong and Privalsky, 2000). Finally, a further consideration raised by the present study is that care should be taken in assuming that a TF requires and can use a specific CoR to repress its targets in a particular tissue simply because it possesses an interaction motif for that CoR.

Acknowledgements

We are indebted to Yang Hong and co-workers for providing the reagents for genomic recombination prior to publication. We thank Stephanie Winter for conducting early studies on salE1 regulation; V. Twombly, T. Schupbach, B. V. Shravage and B. Stronach for advice on, and reagents for, the oogenesis studies; Z. Paroush, S. Shvartsman, Scott Barolo, M. Bienz, the Bloomington and Vienna stock centers and the Developmental Studies Hybridoma Bank for reagents; and A. Hinerman, L. Seebald, J. Kasenchak and R. White for technical assistance. P.U. thanks her Dissertation Committee, K. Arndt, A. VanDemark, M. Schmidt and B. Stronach for advice throughout her graduate career.

Funding

This work was supported by the National Institutes of Health [grant GM079488 to G.C.]. P.U. was supported in part by fellowships from the University of Pittsburgh. Deposited in PMC for release after 12 months.

Competing interests statement

The authors declare no competing financial interests.

Author contributions

P.U. and G.C. designed experiments and wrote the paper. P.U. performed experiments and analyzed data.

Supplementary material

Supplementary material available online at
http://dev.biologists.org/lookup/suppl/doi:10.1242/dev.099366/-/DC1

References

Alexandre, C., Lecourtois, M. and Vincent, J. (1999). Wingless and Hedgehog pattern Drosophila denticle belts by regulating the production of short-range signals. *Development* **126**, 5689-5698.

Barolo, S. and Levine, M. (1997). hairy mediates dominant repression in the Drosophila embryo. *EMBO J.* **16**, 2883-2891.

Barolo, S., Carver, L. A. and Posakony, J. W. (2000). GFP and beta-galactosidase transformation vectors for promoter/enhancer analysis in Drosophila. *Biotechniques* **29**, 726, 728, 730, 732.

Barolo, S., Stone, T., Bang, A. G. and Posakony, J. W. (2002). Default repression and Notch signaling: Hairless acts as an adaptor to recruit the corepressors Groucho and dCtBP to Suppressor of Hairless. *Genes Dev.* **16**, 1964-1976.

Barrio, R. and de Celis, J. F. (2004). Regulation of spalt expression in the Drosophila wing blade in response to the Decapentaplegic signaling pathway. *Proc. Natl. Acad. Sci. USA* **101**, 6021-6026.

Bejsovec, A. and Martinez Arias, A. (1991). Roles of wingless in patterning the larval epidermis of Drosophila. *Development* **113**, 471-485.

Berg, C. A. (2005). The Drosophila shell game: patterning genes and morphological change. *Trends Genet.* **21**, 346-355.

Bianchi-Frias, D., Orian, A., Delrow, J. J., Vazquez, J., Rosales-Nieves, A. E. and Parkhurst, S. M. (2004). Hairy transcriptional repression targets and cofactor recruitment in Drosophila. *PLoS Biol.* **2**, e178.

Campbell, G. and Tomlinson, A. (1999). Transducing the Dpp morphogen gradient in the wing of Drosophila: regulation of Dpp targets by brinker. *Cell* **96**, 553-562.

Chen, Y. and Schüpbach, T. (2006). The role of brinker in eggshell patterning. *Mech. Dev.* **123**, 395-406.

Chen, G., Fernandez, J., Mische, S. and Courey, A. J. (1999). A functional interaction between the histone deacetylase Rpd3 and the corepressor groucho in Drosophila development. *Genes Dev.* **13**, 2218-2230.

Choi, C. Y., Kim, Y. H., Kim, Y. O., Park, S. J., Kim, E. A., Riemenschneider, W., Gajewski, K., Schulz, R. A. and Kim, Y. (2005). Phosphorylation by the DHIPK2 protein kinase modulates the corepressor activity of Groucho. *J. Biol. Chem.* **280**, 21427-21436.

Cinnamon, E., Helman, A., Ben-Haroush Schyr, R., Orian, A., Jiménez, G. and Paroush, Z. (2008). Multiple RTK pathways downregulate Groucho-mediated repression in Drosophila embryogenesis. *Development* **135**, 829-837.

del Álamo Rodríguez, D., Terriente Felix, J. and Díaz-Benjumea, F. J. (2004). The role of the T-box gene optomotor-blind in patterning the Drosophila wing. *Dev. Biol.* **268**, 481-492.

Golembo, M., Raz, E. and Shilo, B. Z. (1996). The Drosophila embryonic midline is the site of Spitz processing, and induces activation of the EGF receptor in the ventral ectoderm. *Development* **122**, 3363-3370.

Gong, W. J. and Golic, K. G. (2003). Ends-out, or replacement, gene targeting in Drosophila. *Proc. Natl. Acad. Sci. USA* **100**, 2556-2561.

Gromöller, A. and Lehming, N. (2000). Srb7p is a physical and physiological target of Tup1p. *EMBO J.* **19**, 6845-6852.

Hasson, P., Müller, B., Basler, K. and Paroush, Z. (2001). Brinker requires two corepressors for maximal and versatile repression in Dpp signalling. *EMBO J.* **20**, 5725-5736.

Hasson, P., Egoz, N., Winkler, C., Volohonsky, G., Jia, S., Dinur, T., Volk, T., Courey, A. J. and Paroush, Z. (2005). EGFR signaling attenuates Groucho-dependent repression to antagonize Notch transcriptional output. *Nat. Genet.* **37**, 101-105.

Hong, S. H. and Privalsky, M. L. (2000). The SMRT corepressor is regulated by a MEK-1 kinase pathway: inhibition of corepressor function is associated with SMRT phosphorylation and nuclear export. *Mol. Cell. Biol.* **20**, 6612-6625.

Huang, J., Zhou, W., Watson, A. M., Jan, Y. N. and Hong, Y. (2008). Efficient ends-out gene targeting in Drosophila. *Genetics* **180**, 703-707.

Huang, J., Zhou, W., Dong, W., Watson, A. M. and Hong, Y. (2009). Directed, efficient, and versatile modifications of the Drosophila genome by genomic engineering. *Proc. Natl. Acad. Sci. USA* **106**, 8284-8289.

Jaźwińska, A., Rushlow, C. and Roth, S. (1999a). The role of brinker in mediating the graded response to Dpp in early Drosophila embryos. *Development* **126**, 3323-3334.

Jaźwińska, A., Kirov, N., Wieschaus, E., Roth, S. and Rushlow, C. (1999b). The Drosophila gene brinker reveals a novel mechanism of Dpp target gene regulation. *Cell* **96**, 563-573.

Jennings, B. H. and Ish-Horowicz, D. (2008). The Groucho/TLE/Grg family of transcriptional co-repressors. *Genome Biol.* **9**, 205.

Jennings, B. H., Wainwright, S. M. and Ish-Horowicz, D. (2008). Differential in vivo requirements for oligomerization during Groucho-mediated repression. *EMBO Rep.* **9**, 76-83.

Keller, S. A., Mao, Y., Struffi, P., Margulies, C., Yurk, C. E., Anderson, A. R., Amey, R. L., Moore, S., Ebels, J. M., Foley, K. et al. (2000). dCtBP-dependent and -independent repression activities of the Drosophila Knirps protein. *Mol. Cell. Biol.* **20**, 7247-7258.

Kim, J. H., Cho, E. J., Kim, S. T. and Youn, H. D. (2005). CtBP represses p300-mediated transcriptional activation by direct association with its bromodomain. *Nat. Struct. Mol. Biol.* **12**, 423-428.

Kühnlein, R. P., Frommer, G., Friedrich, M., Gonzalez-Gaitan, M., Weber, A., Wagner-Bernholz, J. F., Gehring, W. J., Jäckle, H. and Schuh, R. (1994). spalt encodes an evolutionarily conserved zinc finger protein of novel structure which provides homeotic gene function in the head and tail region of the Drosophila embryo. *EMBO J.* **13**, 168-179.

Kühnlein, R. P., Brönner, G., Taubert, H. and Schuh, R. (1997). Regulation of Drosophila spalt gene expression. *Mech. Dev.* **66**, 107-118.

Lammel, U., Meadows, L. and Saumweber, H. (2000). Analysis of Drosophila salivary gland, epidermis and CNS development suggests an additional function of brinker in anterior-posterior cell fate specification. *Mech. Dev.* **92**, 179-191.

Lee, J. R., Urban, S., Garvey, C. F. and Freeman, M. (2001). Regulated intracellular ligand transport and proteolysis control EGF signal activation in Drosophila. *Cell* **107**, 161-171.

Lin, X., Sun, B., Liang, M., Liang, Y. Y., Gast, A., Hildebrand, J., Brunicardi, F. C., Melchior, F. and Feng, X. H. (2003). Opposed regulation of corepressor CtBP by SUMOylation and PDZ binding. *Mol. Cell* **11**, 1389-1396.

Martinez, C. A. and Arnosti, D. N. (2008). Spreading of a corepressor linked to action of long-range repressor hairy. *Mol. Cell. Biol.* **28**, 2792-2802.

Minami, M., Kinoshita, N., Kamoshida, Y., Tanimoto, H. and Tabata, T. (1999). brinker is a target of Dpp in Drosophila that negatively regulates Dpp-dependent genes. *Nature* **398**, 242-246.

Nagel, A. C. and Preiss, A. (2011). Fine tuning of Notch signaling by differential co-repressor recruitment during eye development of Drosophila. *Hereditas* **148**, 77-84.

Nagel, A. C., Krejci, A., Tenin, G., Bravo-Patiño, A., Bray, S., Maier, D. and Preiss, A. (2005). Hairless-mediated repression of notch target genes requires the combined activity of Groucho and CtBP corepressors. *Mol. Cell. Biol.* **25**, 10433-10441.

Nibu, Y., Zhang, H. and Levine, M. (1998a). Interaction of short-range repressors with Drosophila CtBP in the embryo. *Science* **280**, 101-104.

Nibu, Y., Zhang, H., Bajor, E., Barolo, S., Small, S. and Levine, M. (1998b). dCtBP mediates transcriptional repression by Knirps, Krüppel and Snail in the Drosophila embryo. *EMBO J.* **17**, 7009-7020.

Orian, A., Delrow, J. J., Rosales Nieves, A. E., Abed, M., Metzger, D., Paroush, Z., Eisenman, R. N. and Parkhurst, S. M. (2007). A Myc-Groucho complex integrates EGF and Notch signaling to regulate neural development. *Proc. Natl. Acad. Sci. USA* **104**, 15771-15776.

Paroush, Z., Finley, R. L., Jr, Kidd, T., Wainwright, S. M., Ingham, P. W., Brent, R. and Ish-Horowicz, D. (1994). Groucho is required for Drosophila neurogenesis, segmentation, and sex determination and interacts directly with hairy-related bHLH proteins. *Cell* **79**, 805-815.

Payankaulam, S. and Arnosti, D. N. (2009). Groucho corepressor functions as a cofactor for the Knirps short-range transcriptional repressor. *Proc. Natl. Acad. Sci. USA* **106**, 17314-17319.

Poortinga, G., Watanabe, M. and Parkhurst, S. M. (1998). Drosophila CtBP: a Hairy-interacting protein required for embryonic segmentation and hairy-mediated transcriptional repression. *EMBO J.* **17**, 2067-2078.

Rong, Y. S. and Golic, K. G. (2000). Gene targeting by homologous recombination in Drosophila. *Science* **288**, 2013-2018.

Saller, E., Kelley, A. and Bienz, M. (2002). The transcriptional repressor Brinker antagonizes Wingless signaling. *Genes Dev.* **16**, 1828-1838.

Sanson, B. (2001). Generating patterns from fields of cells. Examples from Drosophila segmentation. *EMBO Rep.* **2**, 1083-1088.

Shi, Y., Sawada, J., Sui, G., Affar, B., Whetstine, J. R., Lan, F., Ogawa, H., Luke, M. P., Nakatani, Y. and Shi, Y. (2003). Coordinated histone modifications mediated by a CtBP co-repressor complex. *Nature* **422**, 735-738.

Shravage, B. V., Altmann, G., Technau, M. and Roth, S. (2007). The role of Dpp and its inhibitors during eggshell patterning in Drosophila. *Development* **134**, 2261-2271.

Sivasankaran, R., Vigano, M. A., Müller, B., Affolter, M. and Basler, K. (2000). Direct transcriptional control of the Dpp target omb by the DNA binding protein Brinker. *EMBO J.* **19**, 6162-6172.

Struffi, P. and Arnosti, D. N. (2005). Functional interaction between the Drosophila knirps short range transcriptional repressor and RPD3 histone deacetylase. *J. Biol. Chem.* **280**, 40757-40765.

Struffi, P., Corado, M., Kulkarni, M. and Arnosti, D. N. (2004). Quantitative contributions of CtBP-dependent and -independent repression activities of Knirps. *Development* **131**, 2419-2429.

Subramanian, T. and Chinnadurai, G. (2003). Association of class I histone deacetylases with transcriptional corepressor CtBP. *FEBS Lett.* **540**, 255-258.

Szüts, D., Freeman, M. and Bienz, M. (1997). Antagonism between EGFR and Wingless signalling in the larval cuticle of Drosophila. *Development* **124**, 3209-3219.

Tautz, D. and Pfeifle, C. (1989). A non-radioactive in situ hybridization method for the localization of specific RNAs in Drosophila embryos reveals translational control of the segmentation gene hunchback. *Chromosoma* **98**, 81-85.

Winkler, C. J., Ponce, A. and Courey, A. J. (2010). Groucho-mediated repression may result from a histone deacetylase-dependent increase in nucleosome density. *PLoS ONE* **5**, e10166.
Winter, S. E. and Campbell, G. (2004). Repression of Dpp targets in the Drosophila wing by Brinker. *Development* **131**, 6071-6081.
Xu, T. and Rubin, G. M. (1993). Analysis of genetic mosaics in developing and adult Drosophila tissues. *Development* **117**, 1223-1237.
Yang, L., Meng, F., Ma, D., Xie, W. and Fang, M. (2013). Bridging Decapentaplegic and Wingless signaling in Drosophila wings through repression of naked cuticle by Brinker. *Development* **140**, 413-422.
Zeng, W., Wharton, K. A., Jr, Mack, J. A., Wang, K., Gadbaw, M., Suyama, K., Klein, P. S. and Scott, M. P. (2000). naked cuticle encodes an inducible antagonist of Wnt signalling. *Nature* **403**, 789-795.
Zhang, H. and Emmons, S. W. (2002). Caenorhabditis elegans unc-37/groucho interacts genetically with components of the transcriptional mediator complex. *Genetics* **160**, 799-803.
Zhang, H. and Levine, M. (1999). Groucho and dCtBP mediate separate pathways of transcriptional repression in the Drosophila embryo. *Proc. Natl. Acad. Sci. USA* **96**, 535-540.
Zhang, H., Levine, M. and Ashe, H. L. (2001). Brinker is a sequence-specific transcriptional repressor in the Drosophila embryo. *Genes Dev.* **15**, 261-266.
Zhao, L. J., Subramanian, T., Zhou, Y. and Chinnadurai, G. (2006). Acetylation by p300 regulates nuclear localization and function of the transcriptional corepressor CtBP2. *J. Biol. Chem.* **281**, 4183-4189.
Zhou, W., Huang, J., Watson, A. M. and Hong, Y. (2012). W:Neo: a novel dual-selection marker for high efficiency gene targeting in Drosophila. *PLoS ONE* **7**, e31997.
Ziv, O., Suissa, Y., Neuman, H., Dinur, T., Geuking, P., Rhiner, C., Portela, M., Lolo, F., Moreno, E. and Gerlitz, O. (2009). The co-regulator dNAB interacts with Brinker to eliminate cells with reduced Dpp signaling. *Development* **136**, 1137-1145.

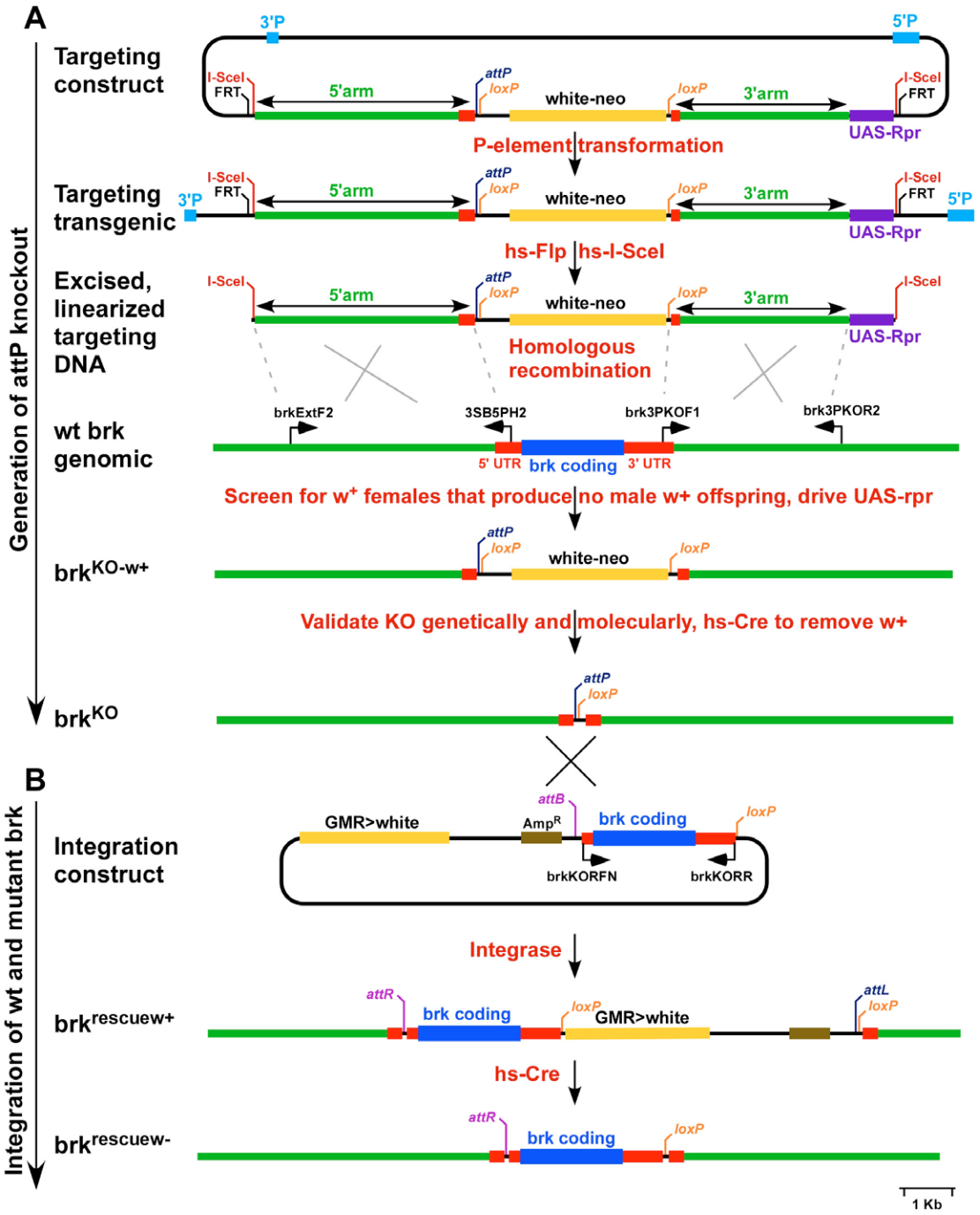

Fig. S1. Generation of endogenous *brk* mutants. This was achieved using the procedures of Golic and Hong and co-workers (Rong and Golic, 2000; Gong and Golic, 2003; Huang et al., 2008; Huang et al., 2009; Zhou et al, 2012) (A) Generation of *brk* knockout (brk^{KO}) by a modified ends out gene targeting approach. A targeting construct was made in vector pGX-PCM1 (this is identical to the pGX-attP-WN vector (Zhou et al, 2012) with the absence of the SphI site) comprising: (i) 5' and 3' *brk* flanking regions/arms extending into the 5' and 3' UTRs (primers for PCR to generate these arms is shown in Fig. S2 and Table S1), (ii) a ØC31 bacteriophage *attP* site positioned 3' to the 5' *brk* arm, (iii) *white* (*w*+) marker flanked by *loxP* sites, positioned between the *brk* arms (iv) UAS-rpr outside of the region containing the arms, to select against non-targeted events, (v) FRT and I-Sce-I sites that flank elements i-iv, and (vi) P-element ends for integration into the genome of *w*- flies. Following P-element mediated-transgenesis, Flippase and I-Sce-I were used to excise and linearize targeting DNA in vivo. Non-targeted events were selected against by crossing to Gal4221[w-] to drive UAS-rpr (which will make such events lethal). 15,000 progeny were screened for *w*+ females (*brk* is on the X) not carrying the original targeting transgene yielding six hundred potential candidates. Out of these ten failed to produce w^+ males and all were characterized as brk KOs molecularly and genetically (Fig. S2, 3) and finally the *w*+ marker was excised using Cre, resulting in the final brk^{KO} in which the *brk* gene is replaced by an *attP* site and *loxP* site.
(B) Integration of wild-type and mutant forms of *brk* into the *attP* site of brk^{KO}. Integration constructs were made consisting of a *brk* gene extending from the regions in the 5' and 3' UTRs not included in the arms used in the targeting construct, the *brk* gene is flanked 5' by an *attB* site and 3' by a *loxP* site, and a *w*+ marker. This is integrated into brk^{KO} using ØC31 integrase and the *w*+ marker is excised from the resulting transformants using Cre resulting in a fly carrying a *brk* gene that is identical to the wild-type with the exception of an *attR* site and *loxP* site in the 5' and 3' UTRs, respectively, along with any modification made to *brk*.

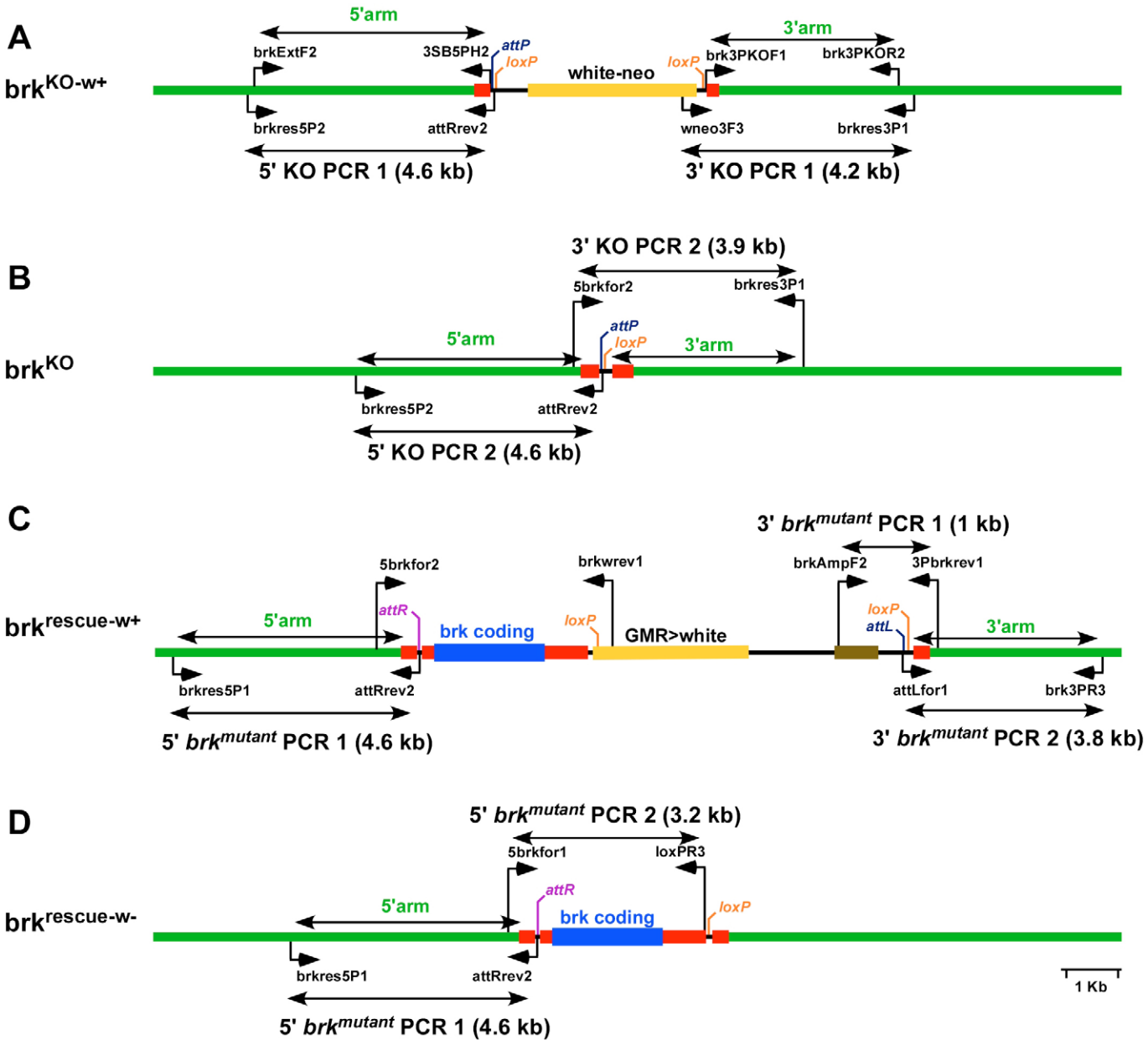

Fig. S2. Molecular validation of *brk*^{KO} and endogenous *brk* mutants. All genotypes indicated were confirmed by PCR amplification of genomic DNA including the novel 5' and 3' ends created by the procedures (expected amplicon size indicated), followed by restriction mapping and sequencing. The PCR was performed with primers outside of those used to generate the arms used in the targeting construct. Validation of the final mutant was also confirmed by amplifying the *brk* gene using a primer in the region including the novel *loxP* sequence in the 3' UTR and a 5' primer outside of the transcription unit. Sequences of primers are listed in Table S1.

Fig. S3. Genetic validation of *brk*^{KO} and restoration of function in *brk*^{rescue}. (A-D) Adult wings. (A) Wild-type with longitudinal veins indicated, L2-L5. (B) The *brk*^{XGXM2} hypomorph has a slightly enlarged posterior, incomplete L5 and a fused alula (arrowed). *brk*^{XGXM2} is a previously unpublished viable allele generated by mobilisation of a P-element insertion, *brk*^{XG} (Campbell, unpublished). (C) The *brk*^{XGXM2} phenotypes are more severe over a null allele, *brk*^{F124}. (D) The *brk*^{XGXM2}/*brk*^{KO} is comparable in severity to the null over *brk*^{XGXM2}. (E) Functional validation of *brk*^{rescue}. The viability of *brk*^{rescue} heterozygotes over a series of embryonic lethal *brk* mutants, *brk*^{M68}, *brk*^{F124}, *brk*^{F138}, *brk*^{E427}, a *brk* deficiency and the larval/pupal lethal *brk*^{XA} was calculated and compared to heterozygotes of a wild-type allele over the same mutants. Although the average is slightly reduced for *brk*^{rescue} heterozygotes, the difference with the wild-type heterozygotes was not significant (n = 3, in each experiment at least 100 females were evaluated, P > 0.05, Mann Whitney U test) indicating that the integration of a wild-type *brk* allele at the deletion locus in the *brk*^{KO} restores and rescues the native *brk* locus functionally.

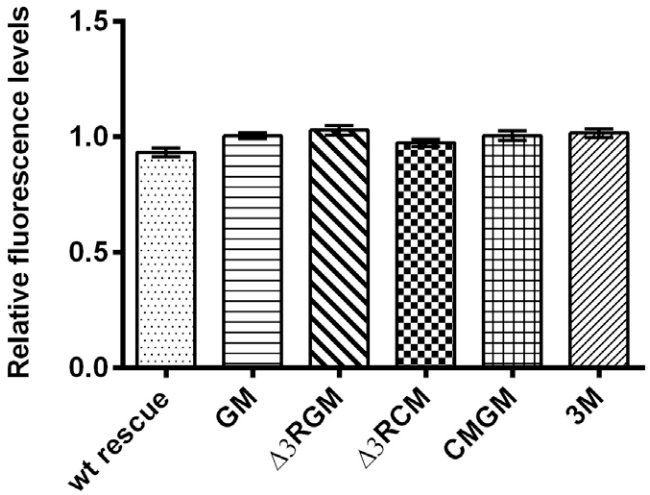

Fig. S4. Comparison of mutant Brk protein levels to wild-type. Wing discs carrying clones of the genotypes indicated were stained with Brk antibody, imaged on a confocal taking care the detector was not saturated and, using ImageJ, the average fluorescence level within a clone situated in the lateral region was compared to the average within an adjacent wild-type twin spot, a value of 1 will then indicate no difference. For every *brk* mutant, twenty independently generated clones were assessed and the average fluorescence level within a clone was measured along with the average within an adjacent wild-type twin spot and the relative difference was calculated; a relative value of 1 will then indicate no difference and a Chi-square test with trend was used to determine whether relative mutant Brk/wild-type levels were significantly different from this 'expected' value. As shown in the scatter-plot the twenty mutant Brk fluorescence values relative to wild-type for every *brk* mutant do not differ significantly from the expected wild-type value of 1, indicated with red dashed line (P > 0.05, chi-square test for trend).

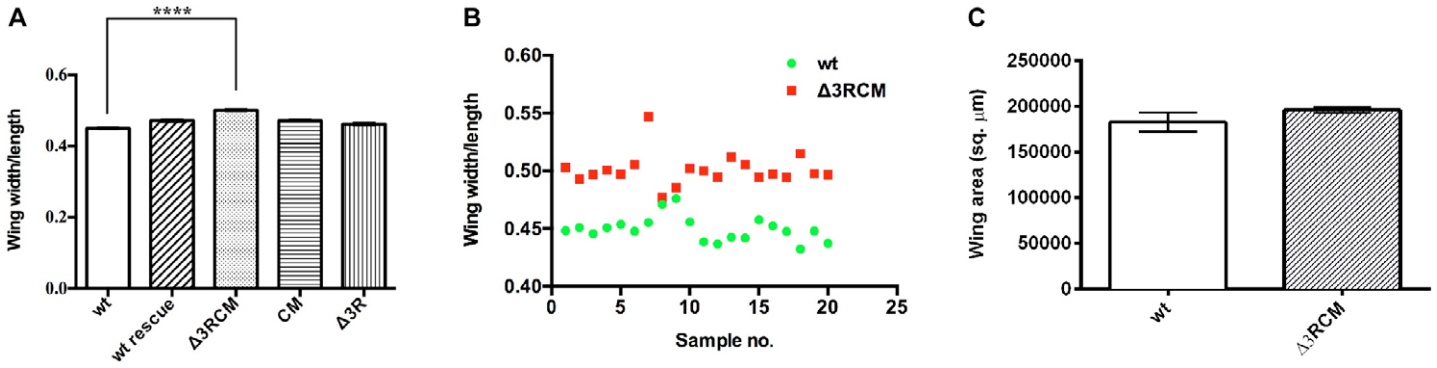

Fig. S5 Comparison of adult wing size in wild-type to that of viable *brk* mutants. (A,B) Ratio of width to length. This ratio for $brk^{\Delta 3RCM}$ wings is slightly, but significantly, higher than wild-type (n = 20, P < 0.0001, Mann Whitney U test) while that of brk^{rescue}, brk^{CM}, $brk^{\Delta 3R}$ is not (n = 10 for each mutant, P > 0.05, Kruskal Wallis test followed by Dunn's multiple comparison). (B) Scatter-plot of the width/length ratios of $brk^{\Delta 3RCM}$ and wild-type wings showing that for a few $brk^{\Delta 3RCM}$ wings the width/length ratio approaches close to the wild-type but is increased for most. (C) The area of $brk^{\Delta 3RCM}$ wings does not vary significantly from the wild-type (n = 20 for each genotype, P > 0.05, Mann Whitney U test).

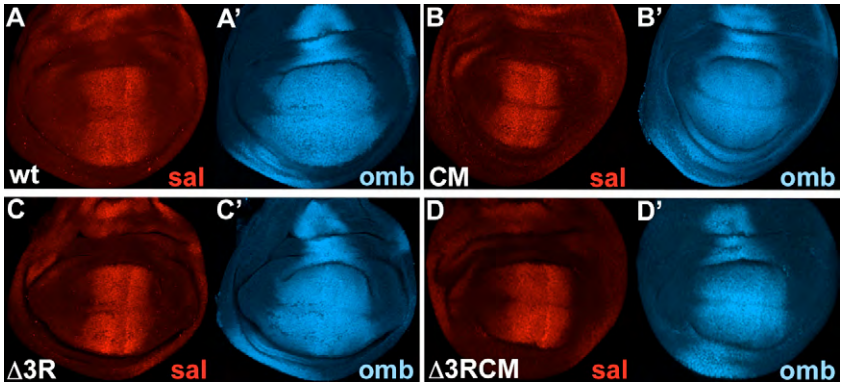

Fig. S6. *sal* and *omb* expression in viable *brk* mutants. Third instar wing discs stained for omb-lacZ (ß-gal antibody) and Sal (antibody), anterior left. Expression of *sal* and ombZ in brk^{CM}, $brk^{\Delta 3R}$, $brk^{\Delta 3RCM}$ (B-D) is indistinguishable from that in the wild-type (A).

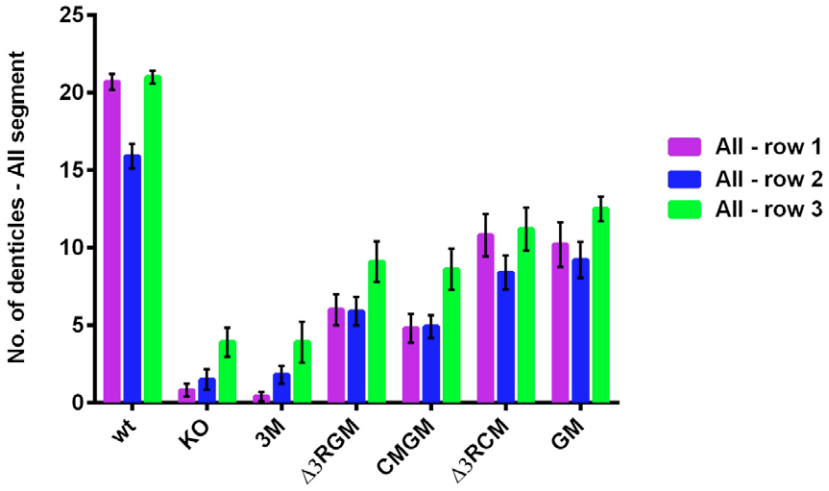

Fig. S7. Comparison of the number of denticles in rows 1-3 of the VDB of the second abdominal segment (AII) in wild-type and *brk* mutants. Number of denticles remaining in rows 1-3 of AII ventral denticle belt are in significantly reduced in the following *brk* mutants, brk^{KO}, brk^{3M}, $brk^{\Delta 3RGM}$, brk^{CMGM}, $brk^{\Delta 3RCM}$ and brk^{GM} (n = 10, P < 0.01, Mann Whitney U test). The loss of denticles is most severe in brk^{KO} and brk^{3M}, of intermediate severity in $brk^{\Delta 3RGM}$ and brk^{CMGM} and milder in brk^{GM} and $brk^{\Delta 3RCM}$. All mutants except $brk^{\Delta 3RCM}$ display a polarity defect, such that all the remaining denticles point posteriorly compared to the wild-type where denticles in rows 1 and 4 point anteriorly while rest point posteriorly.

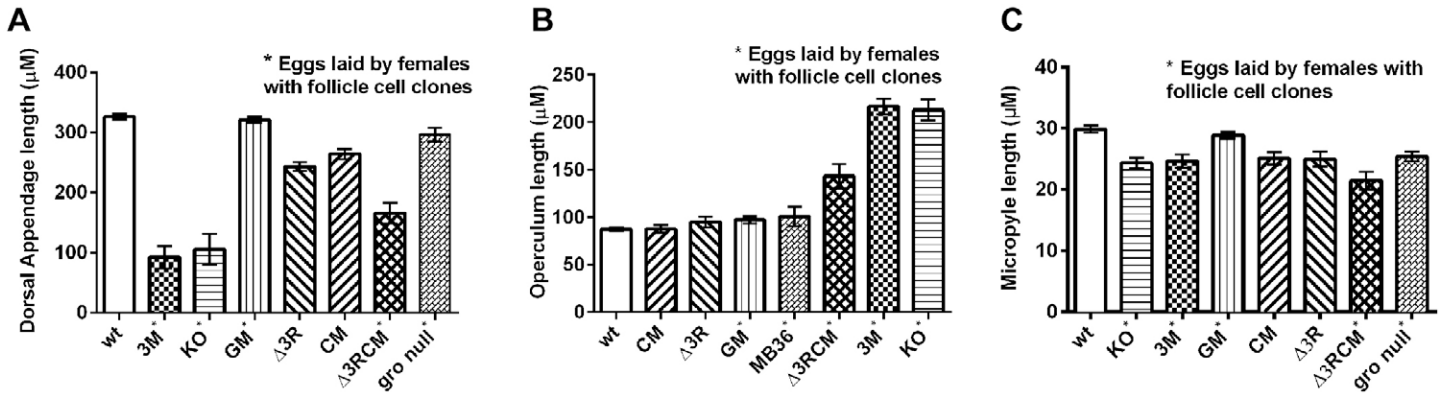

Fig. S8. Size of the dorsal appendages (DAs), operculum and micropyle in eggs laid by mutant mothers or mothers carrying follicle cell clones. Eggs laid by mothers with follicle cell clones are marked with * Compared to wild-type, eggs from mothers carrying brk^{KO} and brk^{3M} follicle cell clones have (A) only one reduced or no DAs ($P < 0.0001$), (B) the opercula are significantly larger ($P < 0.0001$) and (C) the micropyle are significantly reduced ($P < 0.01$). Eggs from brk^{CM} and $brk^{\Delta 3R}$ homozygous mothers have (A) significantly shorter DAs ($n = 10$, $P < 0.0001$), (B) opercula appear wild-type ($n = 10$, $P > 0.05$) and (C) micropyle are reduced ($n = 10$, $P < 0.01$). Eggs from mothers carrying $brk^{\Delta 3RCM}$ follicle cell clones have (A) significantly shorter or no DAs ($P < 0.0001$) occasionally being as severe as brk^{KO}, (B) opercula that are significantly expanded ($P < 0.0001$) and (C) reduced micropyle ($P < 0.01$). Eggs from mothers carrying brk^{GM} follicle cell clones have (A) wild-type DAs ($P > 0.05$), (B) slightly expanded opercula ($P < 0.05$) and (C) wild-type micropyle ($P > 0.05$). Eggs from mothers carrying follicle cell clones of the *gro* null allele, gro^{MB36} have (A) shorter DAs compared to wild-type ($n = 10$, $P < 0.01$), (B) wild-type opercula ($n = 10$, $P > 0.05$) and (C) reduced micropyle ($P < 0.01$). P values calculated using the Mann Whitney U test, $n = 20$ unless indicated.

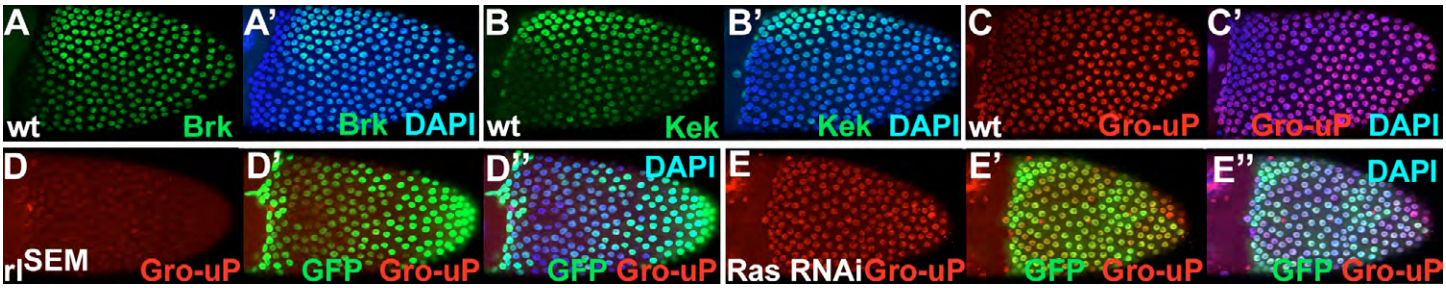

Fig. S9. Gro phosphorylation by EGFR signaling in the follicular epithelium. Duplication of egg chambers in Fig. 8, now showing DAPI and UAS-GFP.

Table S1. Primers used in PCR to generate homology arms and to amplify genomic DNA from mutants

Primer	Sequence
brkExtF2	atgcggtaccCAAGTCAAGATGGCTTGC
3SB5PH2	gatcggtaccTCATAACTCGCGATCTGG
brk3PKOF1	gatccctaggATGCGCCTATACATAGAG
brk3PKOR2	gatccctaggGTGTTCGTGTCAATGTGTGC
brkres5P2	gatcCAGCATTTTGATATAAATTTATC
attRrev2	gatcGTTACCCCAGTTGGGGCACTAC
wneo3F3	CTGTTTATTGCCCCCTCAAA
brkres3P1	gatcCGCGTGCGTGTATATTTATG
5brkfor2	gatcGTGCCAGTGTGTGTATGTG
brkres5P1	gatcGAATGCTCAAGAGACGTG
brkwrev1	gatcGAGGGAGAGTCACAAAACG
brkAmpF2	gatcCTGGTGAGTACTCAACCAAG
3Pbrkrev1	gatcGTATAGGCGCATTCCTAGGC
attLfor1	gatcCTCTCAGTTGGGGGCGTAG
brk3PR3	GCCCTATGTTTTGCCCAGT
5brkfor1	gatcCACAACTATATAGATTTGAAAC
loxPR3	GAAGTTATGGTACCTTAATATTTC

See Fig. S2 for location of primers.